arXiv:gr-qc/0605104v1 18 May 2006

Embedding the Reissner-Nordström spacetime in Euclidean and Minkowski spaces

Uri Jacob and Tsvi Piran

Racah Institute of Physics, Hebrew University, Jerusalem, Israel

E-mail: uriyada@phys.huji.ac.il, tsvi@phys.huji.ac.il

Abstract. We examine embedding diagrams of hypersurfaces in the Reissner-Nordström black hole spacetime. These embedding diagrams serve as useful tools to visualize the geometry of the hypersurfaces and of the whole spacetime in general.

PACS numbers: 04.20.-q, 04.20.Jb, 04.70.Bw

1. Introduction

The Reissner-Nordström (RN) spacetime describes a vacuum where matter and electric charge exist in a singularity at the center ($r = 0$). When the mass is large enough compared to the electric charge, $M > Q$, which is the case we explore here, a black hole engulfs the singularity. This black hole is far more complex than the simple Schwarzschild black hole.

The RN spacetime has been extensively investigated in the past (see e.g. [1, 2, 3]). Our aim here is to describe the embedding diagrams of typical hypersurfaces of this spacetime. The embedding diagrams of spatial hypersurfaces of the Schwarzschild black hole are well known (see [1]). Surprisingly, little is known about the corresponding diagrams of the richer RN (and the rather similar Kerr) spacetime. We review briefly the concept of embedding diagrams in Sec. 2 and discuss as an example the embedding of the Schwarzschild spacetime. We present in Sec. 3 RN coordinate systems that enable us to explore the RN spacetime, and we derive the formulas to calculate the embeddings of RN hypersurfaces. In Sec. 4 we present the embedding diagrams of these slices. We summarize our results in Sec. 5.

2. Embedding diagrams

Embedding diagrams of hypersurfaces of a spacetime are useful tools to visualize the overall geometry. Consider a 3-dimensional hypersurface with an induced metric of $ds^2 = \tilde{g}_{ij}dx^i dx^j$. When the hypersurface is spherically symmetric (and $r \neq const$ on the

hypersurface), we can select a 2-dimensional plane within this hypersurface and express the metric as:

$$ds^2 = \tilde{g}_{rr}dr^2 + r^2 d\varphi^2. \tag{1}$$

This 2-dimensional plane can now be embedded in a flat 3-dimensional space:

$$ds^2 = \pm dz^2 + dr^2 + r^2 d\varphi^2. \tag{2}$$

This embedding space is Euclidean or Minkowski depending on whether $\tilde{g}_{rr} \gtrless 1$ (see (3)). The embedding diagram is described by the embedding function $z(r)$, such that the surface $z(r)$ has the same intrinsic geometry as the original spacetime slice:

$$z(r) = \int \sqrt{\pm(\tilde{g}_{rr} - 1)}dr \tag{3}$$

where the $\pm$ signs are for Euclidean and Minkowski embeddings respectively. Timelike hypersurfaces ($ds^2 < 0$), which imply $\tilde{g}_{rr} < 0$ everywhere, are always embedded in Minkowski space, whereas certain spacelike hypersurfaces ($ds^2 > 0$) are embedded in Euclidean space and others in Minkowski space.

In 1916 Flamm [4] had already obtained the well known Schwarzschild "wormhole" with an analytic embedding function of $z = [8M(r - 2M)]^{\frac{1}{2}}$. This describes a hypersurface of $t = const$ outside the event horizon, and similar embeddings correspond to horizontal lines, $v = const$, in the Kruskal-Szekeres coordinates. An embedding diagram of such a hypersurface is displayed in figure 1. The less familiar embedding of the $t = const$ hypersurface inside the Schwarzschild event horizon ($r < 2M$) is presented in figure 2. This is a timelike hypersurface (described by a vertical line, $u = const$, in the Kruskal-Szekeres coordinates), and its embedding is in Minkowski space. Since our spacetime slices always have an axial symmetry, we will use in the following only 2-dimensional diagrams such as figure 2 to describe our surfaces. We adopt here a convention that when the embedding space is Minkowski the diagram is described by a dashed line, while it is a solid line in Euclidean space.

3. The coordinate systems

The familiar RN metric is described in Schwarzschild-like coordinates as:

$$ds^2 = -\left(1 - \frac{2M}{r} + \frac{Q^2}{r^2}\right)dt^2 + \left(1 - \frac{2M}{r} + \frac{Q^2}{r^2}\right)^{-1} dr^2 + r^2(d\theta^2 + sin^2\theta d\varphi^2) \tag{4}$$

where the parameters M and Q describe the mass and electric charge. We consider here $M > |Q|$ when a black hole exists. In this case we have two horizons:

$$r_\pm = M \pm \sqrt{M^2 - Q^2} \tag{5}$$

We get rid of the coordinate singularities on $r_\pm$ by moving to a Kruskal-Szekeres-like coordinate system:

$$ds^2 = f(r)(-d\psi^2 + d\xi^2) + r^2(d\theta^2 + sin^2\theta d\varphi^2) \tag{6}$$

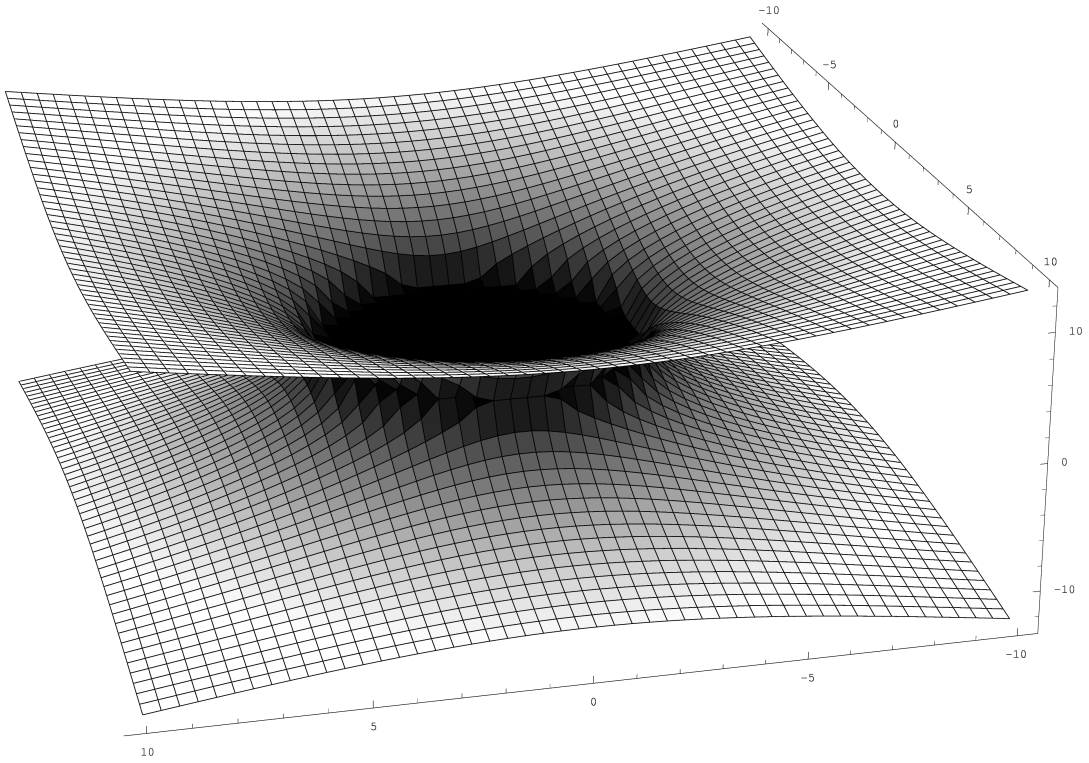

Figure 1. An embedding diagram in Euclidean space of a Schwarzschild spacetime hypersurface described by a horizontal line in the Kruskal-Szekeres coordinates. This surface displays a spacelike wormhole. The diagram shows the vertical embedding lift z as a function of the r, φ coordinates (the $x - y$ plane).

where $f(r) > 0$. In fact we use two separate coordinate systems - coordinate system A that is analytic at r_+ but singular at r_- and coordinate system B that is analytic at r_- but singular at r_+. The coordinate transformations from r, t to ξ, ψ will take a different form in the three regions of spacetime:

$$\begin{aligned} I: &\qquad r > r_+ \\ II: &\ r_- < r < r_+ \\ III: &\qquad r < r_- \end{aligned}$$

We will use system A to describe regions I and II and system B to describe regions II and III. The transformations to coordinate systems A,B in regions I, II, III are:

$$\begin{Bmatrix} \xi_{A,I} \\ \xi_{A,II} \\ \xi_{B,II} \\ \xi_{B,III} \end{Bmatrix} = \begin{Bmatrix} C(r) \\ C(r) \\ C(r)^{-1} \\ -C(r)^{-1} \end{Bmatrix} \begin{Bmatrix} \cosh[F(t)] \\ \sinh[F(t)] \\ \sinh[F(t)] \\ \cosh[F(t)] \end{Bmatrix} \tag{7a}$$

$$\begin{Bmatrix} \psi_{A,I} \\ \psi_{A,II} \\ \psi_{B,II} \\ \psi_{B,III} \end{Bmatrix} = \begin{Bmatrix} C(r) \\ C(r) \\ -C(r)^{-1} \\ C(r)^{-1} \end{Bmatrix} \begin{Bmatrix} \sinh[F(t)] \\ \cosh[F(t)] \\ \cosh[F(t)] \\ \sinh[F(t)] \end{Bmatrix} \tag{7b}$$

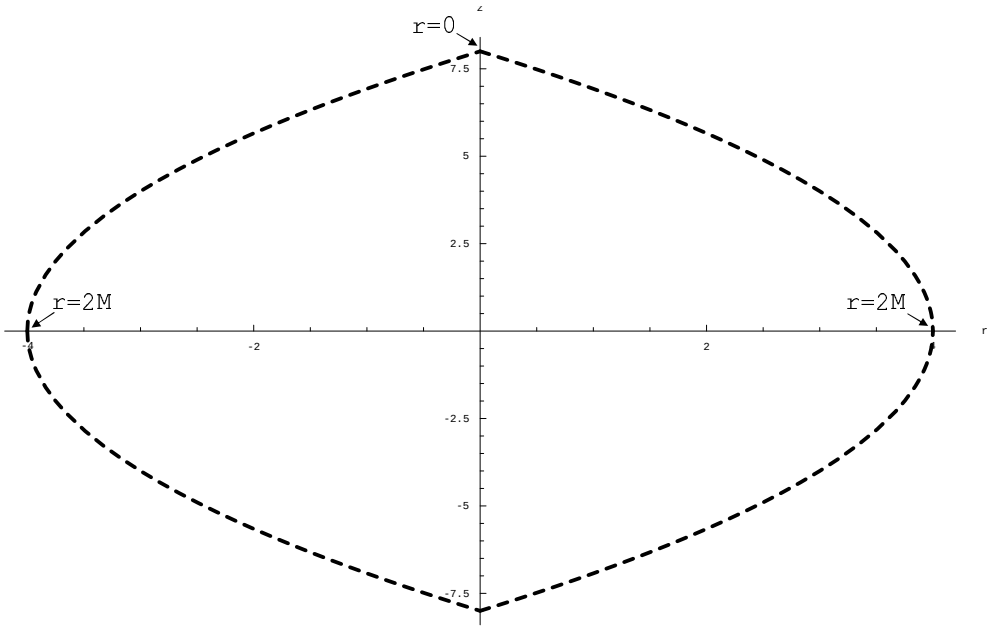

Figure 2. An embedding diagram in Minkowski space of a timelike Schwarzschild spacetime hypersurface described by a vertical line in the Kruskal-Szekeres coordinates. Here we discard of the symmetric φ coordinate and display the embedding lift as a function of r alone. The left half of the diagram does not refer of course to negative r's - it is merely a rotation of 180° that is shown in order to ease the visualization of the entire surface. This embedding is denoted by a dashed line to indicate the background Minkowski space.

where

$$F(t) \equiv \frac{\sqrt{M^2 - Q^2}}{r_+^2} t \tag{8}$$

and

$$C(r) \equiv \left| \frac{r - r_+}{2M} \right|^{\frac{1}{2}} \left| \frac{r - r_-}{2M} \right|^{-\frac{r_-^2}{2r_+^2}} \exp\left[\frac{\sqrt{M^2 - Q^2}}{r_+^2} r \right]. \tag{9}$$

$C(r)$ is an analytic function in each region of spacetime, and r is expressed implicitly in terms of the new coordinates using:

$$\xi^2 - \psi^2 = \pm C(r)^{\pm 2} \tag{10}$$

where the appropriate $\pm$ signs for each region and coordinate system is determined by (7). We use in the following lower indexes to indicate the coordinate system and region to which we refer.

Figure 3 depicts constant r lines in the ξ, ψ plane of coordinate system A. The transformations presented in (7) are valid for one set of system A regions - the upper right half of figure 3 corresponding to $\xi > |\psi|$ or $\psi > |\xi|$. A parallel set of regions with identical geometries is obtained by similar transformations ($\xi_A \to -\xi_A,\ \psi_A \to -\psi_A$).

Figure 4 shows constant r lines in the ξ_B, ψ_B plane. The system B transformations in (7) describe the lower left half of figure 4, and again the parallel regions are similarly

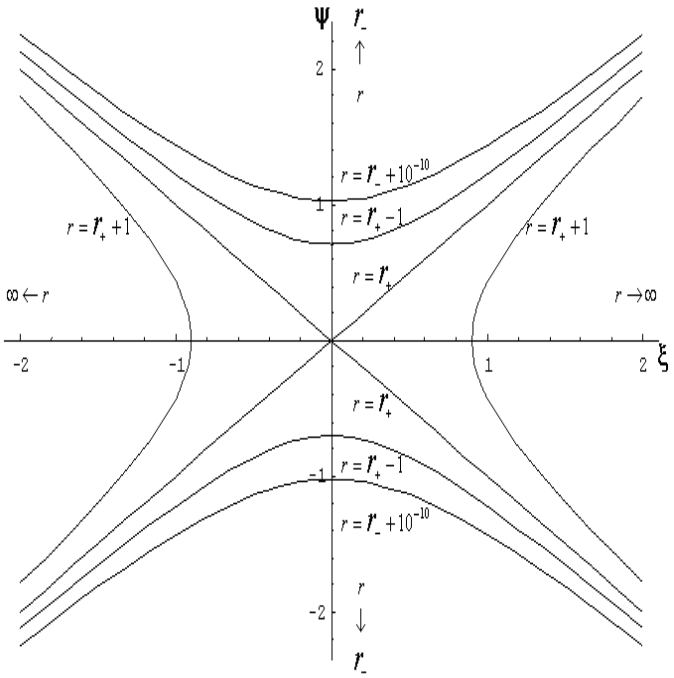

Figure 3. Coordinate system A, analytic around the r_+ horizon. The relation between the original radial coordinate and the new coordinates is displayed for an example of a black hole characterized by $M = 2$, $Q = 1$. $r = const$ hypersurfaces appear here as hyperbolae with the asymptotes $\psi = \pm\xi$. These asymptotes describe the surfaces $r = r_+$, while the surfaces $r = r_-$, which are singular in the current coordinates, are located at the upper and lower infinity of this diagram (where $\xi^2 - \psi^2 = -\infty$).

obtained. The two separate coordinate systems connect of course as ψ goes to $\pm\infty$, demonstrating the known structure of the RN spacetime, which is in essence an infinite chain of parallel asymptotically flat universes connected by wormholes.

We consider embedding diagrams of spacelike and timelike hypersurfaces that are described by horizontal and vertical lines in the ξ, ψ coordinate systems. Horizontal lines mean $d\psi = 0$, which implies in coordinate system A:

$$\left\{ \begin{array}{c} dt_I \\ dt_{II} \end{array} \right\} = - \left\{ \begin{array}{c} \tanh[F(t)] \\ \coth[F(t)] \end{array} \right\} \left(1 - \frac{2M}{r} + \frac{Q^2}{r^2} \right)^{-1} dr \tag{11}$$

Using (3), the embedding function of such a hypersurface in Euclidean (+) or Minkowski (−) space is given by:

$$\left\{ \begin{array}{c} z(r)_I \\ z(r)_{II} \end{array} \right\} = \int \sqrt{ \pm \left(\frac{2M}{r} - \frac{Q^2}{r^2} - \left\{ \begin{array}{c} \tanh^2[F(t)] \\ \coth^2[F(t)] \end{array} \right\} \right) \left(1 - \frac{2M}{r} + \frac{Q^2}{r^2} \right)^{-1} } dr \tag{12}$$

Repeating this procedure for horizontal lines in region II of coordinate system B we get the same embedding formula as the one for coordinate system A in (12). The embedding function of horizontal lines in region III of coordinate system B is identical to the one for

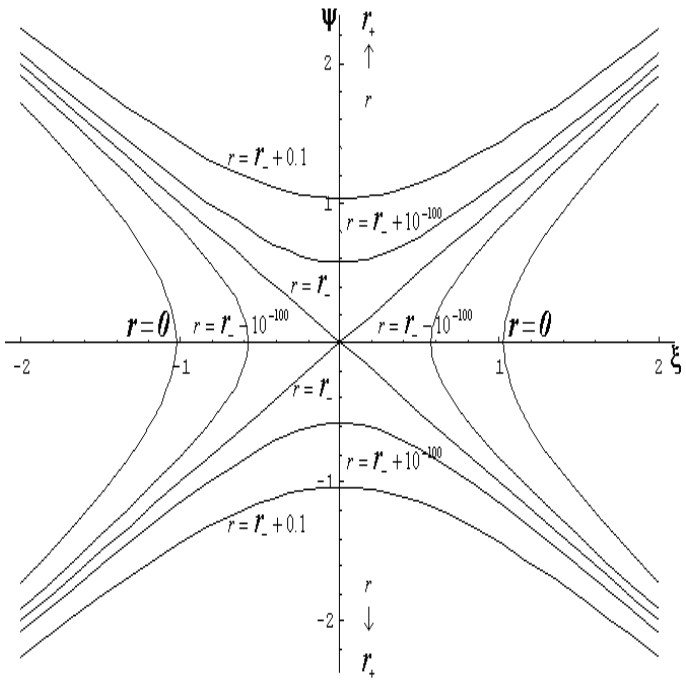

Figure 4. Coordinate system B, analytic around the r_- horizon. The relation between r and the new coordinates is displayed for an example of $M = 2$, $Q = 1$. $r = const$ hypersurfaces appear here as hyperbolae with the asymptotes $\psi = \pm\xi$. These asymptotes describe the surfaces $r = r_-$, while the surfaces $r = r_+$, which are singular in the current coordinates, are located at the upper and lower infinity of this diagram.

region I in (12). The difference is that the parameter t is assigned different values than before, as it is determined by solving the equation $\psi_B = const$ rather than $\psi_A = const$.

We can similarly arrive at the expressions for embedding surfaces of vertical lines ($d\xi = 0$). Such a vertical line is partly described by coordinate system A and partly described by coordinate system B. In order to get the entire embedded surface (which passes through regions I, II and III) we need to connect continuously and smoothly the embedding curves of the two coordinate systems. Note that due to the different coordinate transformations, straight lines of $\xi = const$ in coordinate system A do not necessarily connect with straight lines of the same $\xi = const$ in coordinate system B. Once we choose the connection point between r_- and r_+, we are required to match the same spacetime event in both coordinate systems, determining specific sets of vertical lines. Regardless of this arbitrariness, the embedding diagrams show the qualitative features of timelike and spacelike hypersurfaces, and the arbitrary details of the specific hypersurfaces are not important. The embedding functions we get in Minkowski space (timelike surfaces can never be embedded in Euclidean space) are:

$$\left\{ \begin{array}{c} z(r)_I \\ z(r)_{II} \\ z(r)_{III} \end{array} \right\} = \int \sqrt{-\left(\frac{2M}{r} - \frac{Q^2}{r^2} - \left\{ \begin{array}{c} \coth^2[F(t)] \\ \tanh^2[F(t)] \\ \coth^2[F(t)] \end{array} \right\} \right) \left(1 - \frac{2M}{r} + \frac{Q^2}{r^2} \right)^{-1}} dr \quad (13)$$

where t is determined by coordinate system A's transformation for region I and by coordinate system B's transformation for region III. For region II t can be determined by either systems' transformations, depending on our choice of the vertical lines' connection point.

4. The embedding diagrams of RN hypersurfaces

Using the tools developed in the previous section we turn now to the embedding diagrams of different hypersurfaces in the RN spacetime. Figure 5 depicts a Penrose diagram of the RN spacetime (as shown in [5]). We sketch on this diagram lines corresponding to

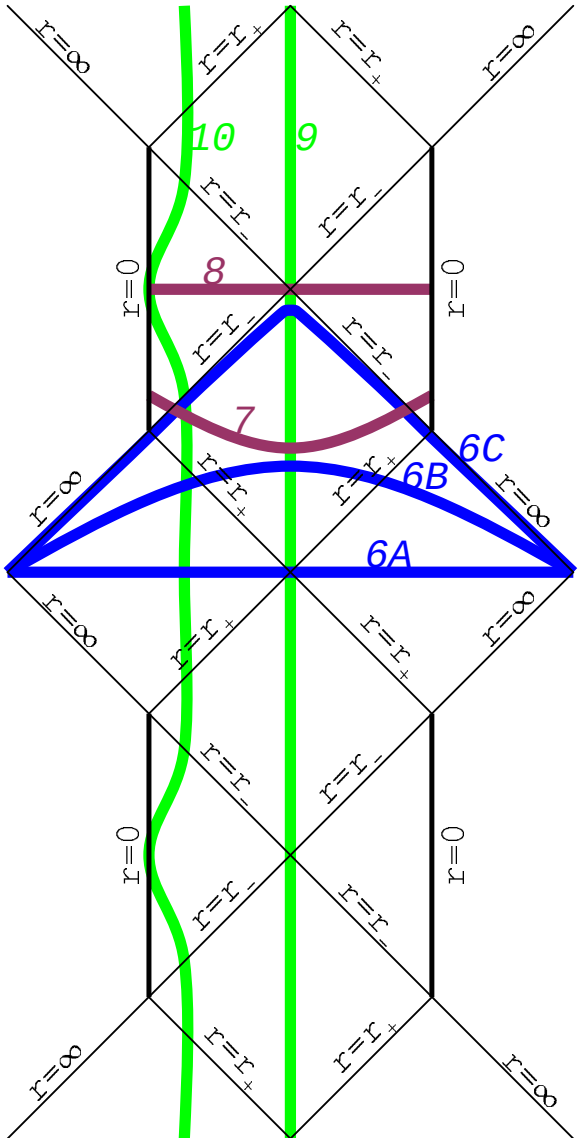

Figure 5. A Penrose diagram of the RN spacetime. The thick lines describe the hypersurfaces, whose embedding diagrams we display. The numbering corresponds to the embedding figures' numbers. While the straight lines *(6A,8,9)* provide an accurate description of the embedded surfaces, the other lines are schematic.

the hypersurfaces for which we present embedding diagrams in this section. We use as an example throughout the discussion here the case $M = 2,\ Q = 1$.

We begin with spacelike hypersurfaces presented as horizontal lines in coordinate system A. The line element of the $\psi = 0$ surface is the same as any $t = const$ surface ($r > r_+$) in the original r, t coordinates. We expect this surface to be similar to that of $t = const,\ r > 2M$ in the Schwarzschild spacetime, as both cases describe a spacelike wormhole connecting at the event horizon two asymptotically flat regions. The spacetime geometry is independent of the t coordinate, but t becomes a spacelike coordinate when crossing the event horizon. This means that for an observer looking at the black hole from outside the spacetime appears static. To explore the geometry seen by an observer who crosses the event horizon and journeys into the black hole we advance with the ψ coordinate, which is a genuine timelike coordinate in all regions, and inspect the evolution of the spacelike hypersurfaces with $\psi = const > 0$.

Figure 6 depicts the embedding diagrams of the $\psi_A = 0$, $\psi_A = 0.8$ and $\psi_A = 1$ hypersurfaces. The geometry of the different surfaces varies. This demonstrates the

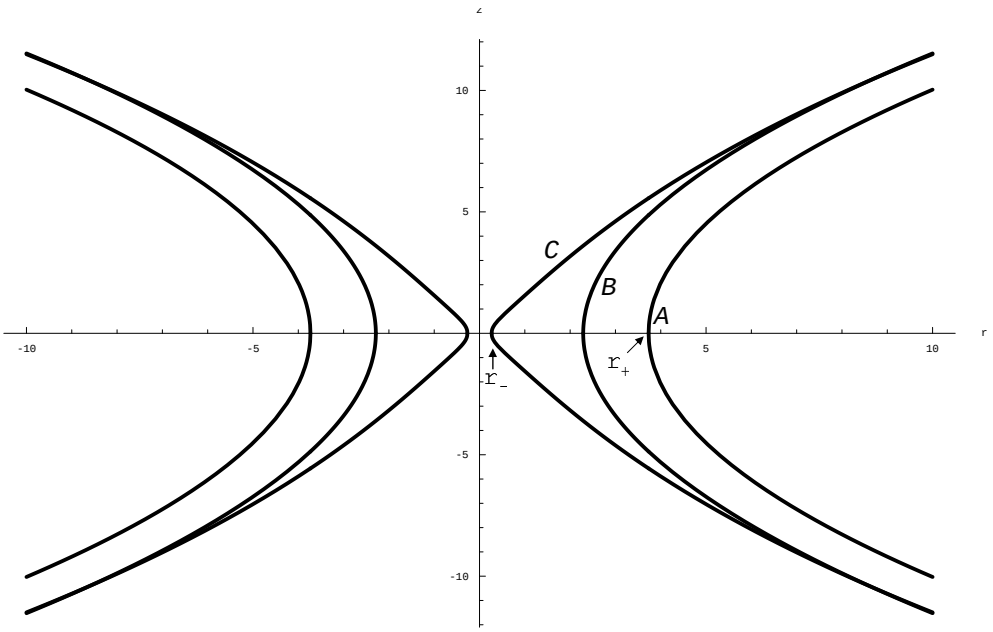

Figure 6. Embedding diagrams in Euclidean space of spacelike RN hypersurfaces described by horizontal lines in coordinate system A. These embeddings display the evolving nature of the spacelike wormhole. Curve A describes the $\psi = 0$ surface where the wormhole is widest. Curve B describes the $\psi = 0.8$ surface, and curve C belongs to the $\psi = 1$ surface, which nearly describes the wormhole of smallest circumference.

fact that the RN spacetime is actually dynamic. As we advance in ψ_A the wormhole shrinks. This phenomena also occurs when advancing along the timelike Kruskal-Szekeres coordinate in the Schwarzschild spacetime. While r_- is reached only as $\psi_A \to \infty$, the surface described by $\psi_A = 1$ can be treated with our working accuracy as if it is tangent to the $r = r_-$ hyperbola (see figure 3). The wormhole with a throat radius of r_- is the narrowest wormhole that the time evolution in coordinate system

A allows. This is contrary to the Schwarzschild case, where the wormhole continues to shrink until it closes when reaching the singularity.

To explore further the RN spacetime we must transform to coordinate system B. Horizontal lines in this coordinate system describe spacelike hypersurfaces that begin at the $r = 0$ singularity and increase in radial distance until connecting with the parallel region after crossing the r_- horizon. Therefore the embedding diagrams of these hypersurfaces will be of a different nature. In the proximity of the $r = 0$ singularity we can never embed any surface in Euclidean space. The RN line element (4) has $g_{rr} \to 0$ and $g_{tt} \to -\infty$ as $r \to 0$. Every path that approaches $r = 0$ will have at a sufficiently small radius $\tilde{g}_{rr} < 1$. Therefore around the singularity we must embed the following surfaces in Minkowski space. At a certain distance the embedding becomes Euclidean. As we examine the evolution of spacelike surfaces seen by a traveler that enters the black hole, we enter coordinate system B from the bottom and draw in figure 7 the embedding diagram of the surface described by $\psi_B = -1.19$. The connection between the parallel

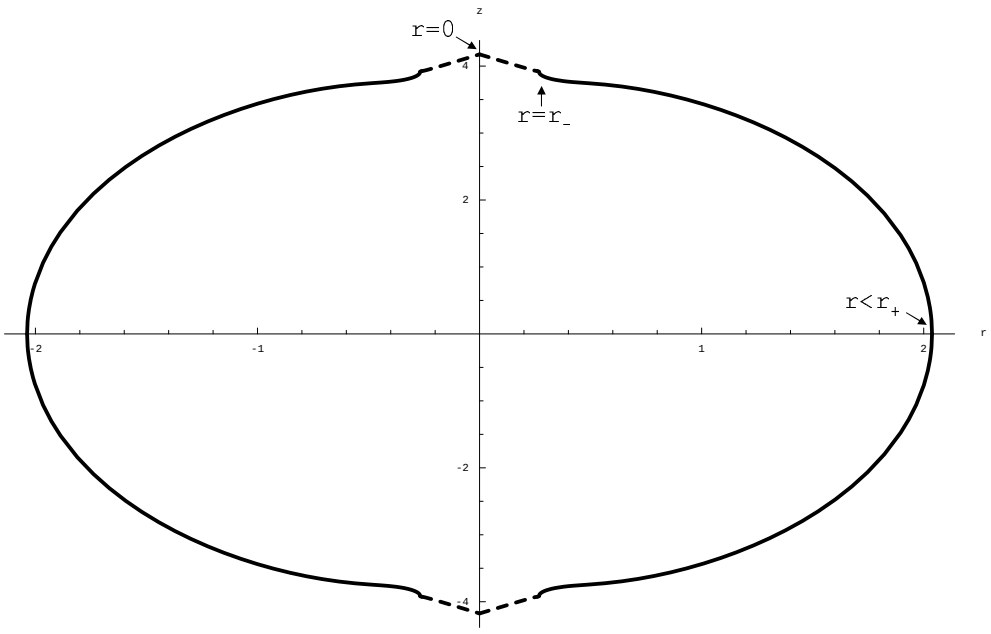

Figure 7. The embedding diagram of the $\psi_B = -1.19$ hypersurface. For brevity the figure depicts two different surfaces that describe the embeddings of parts of this hypersurface in different background spaces. The portion described by dashed lines is embedded in Minkowski space and the portion described by solid lines is embedded in Euclidean space. We can see an inflection point at $r = r_-$. Note that the Minkowski portion starts at $r < r_-$.

regions ($z = 0$) occurs now when increasing the radial distance (up to $r = 2 < r_+$ in the example above). Figure 4 shows that the two inner parallel regions are "closest" in the surface of $\psi_B = 0$, where they touch at $r = r_-$. The embedding of this surface is displayed in figure 8.

It is interesting to inspect the resemblance between the geometry of the horizontal lines in coordinate system B and the geometry of the vertical lines in the Kruskal-

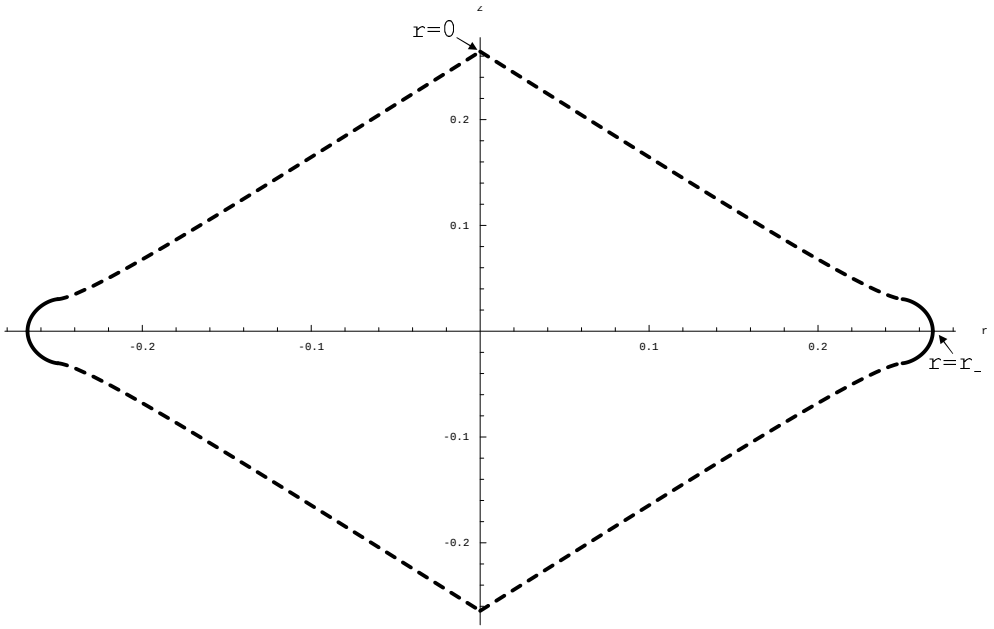

Figure 8. The embedding diagram of the $\psi_B = 0$ hypersurface. For brevity, here again, the figure depicts two different surfaces that describe the embeddings of parts of this hypersurface in different background spaces.

Szekeres coordinates of the Schwarzschild spacetime. We can imagine a resemblance because the Schwarzschild spacetime's vertical lines also emerge from the $r = 0$ singularity and connect with a parallel region after crossing the horizon. However, these vertical lines describe timelike hypersurfaces and so their embeddings will all be in Minkowski spaces. Comparing figures 7,8 with figure 2, we indeed see some resemblance. The region near the singularity in the RN spacetime's horizontal lines has a similar general shape to the Schwarzschild spacetime's vertical lines on their way from the singularity to the parallel region. The region in RN with $r > r_-$ continues towards the parallel region like the Schwarzschild surfaces, but this region is embedded in Euclidean space while the Schwarzschild surfaces continue in Minkowski space.

We turn now to inspect timelike hypersurfaces of the RN spacetime described by vertical lines in our coordinate systems. The $\xi = 0$ line passes in the two coordinate systems only in regions II between $r = r_-$ and $r = r_+$. The embedding diagram of this surface (in Minkowski space of course) is displayed in figure 9. We can see in the figure a connection (the timelike wormhole presented in coordinate system B) between parallel regions at $r = r_-$. Additionally, we can see in coordinate system A a timelike wormhole connecting parallel regions at $r = r_+$, and this should be visible in the embedding by connecting the upper and lower ends of figure 9 with identical diagrams. The complete surface is achieved by connecting an infinite chain of such diagrams. When passing through the r_- horizon to a parallel region there appears to be a cusp in the embedding. This is not a consequence of performing a wrong connection between the coordinate systems, since the entire calculation here was done in a single coordinate system. However, a close inspection of the embedding function reveals that

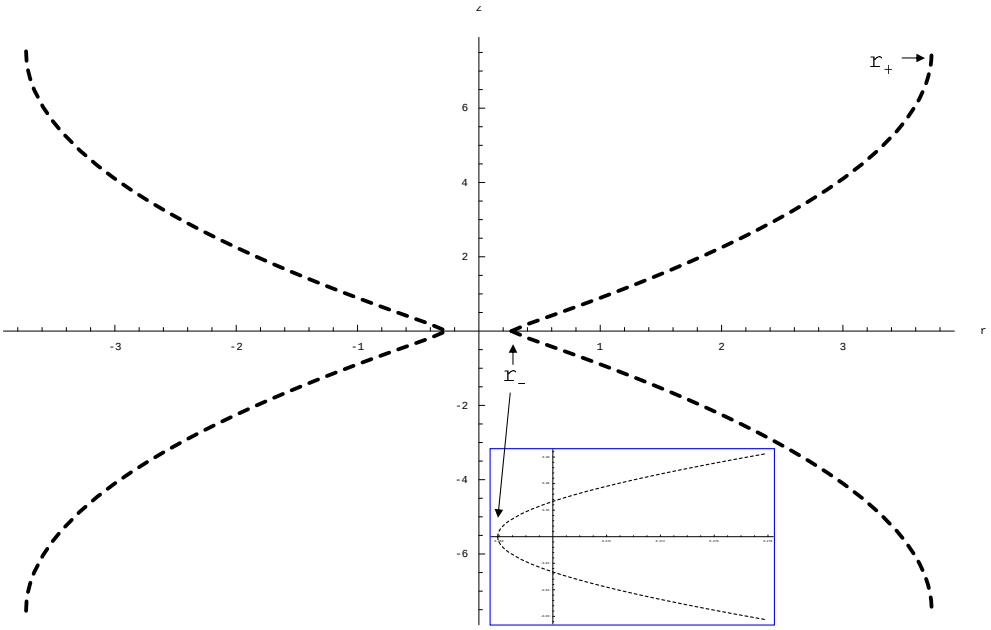

Figure 9. The Minkowski embedding of the $\xi = 0$ hypersurface. The diagram shows just one of the periodic segments of the infinite surface. The enlargement demonstrates the smoothness of the embedding at the r_- wormhole throat.

its slope is in fact continuous at $r = r_-$. When approaching the wormhole throat at r_-, z' diverges, as is required for a smooth connection (see the inset in figure 9).

We now move the vertical line to the side (either positive or negative ξ) and examine a hypersurface that touches the singularity at $r = 0$ (see figure 10). This timelike

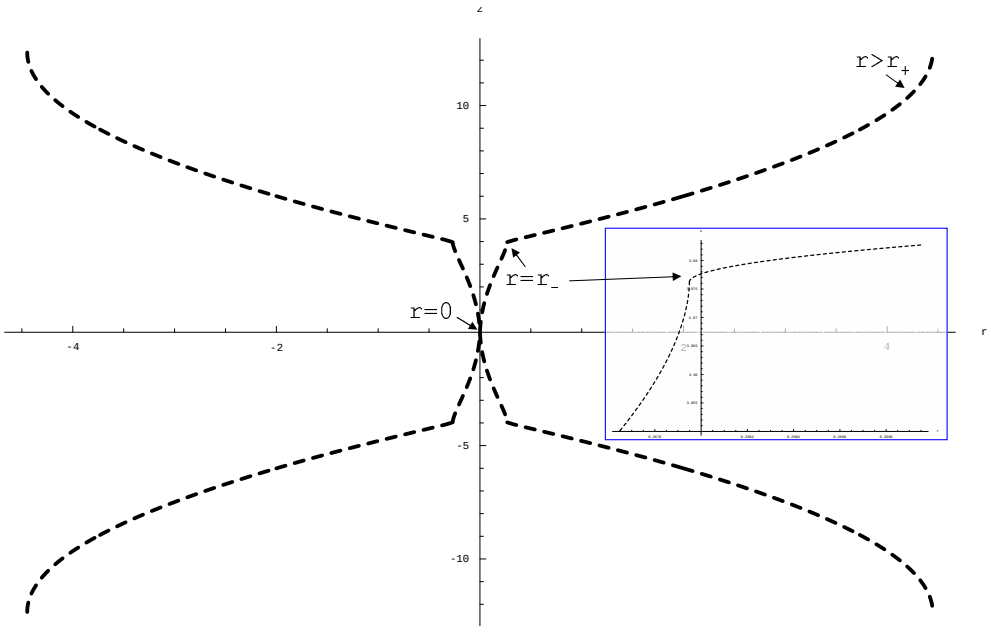

Figure 10. The Minkowski embedding of a timelike hypersurface described by a vertical line that is tangent to the $r = 0$ surface.

surface passes regions I, II and III. It begins by touching the $r = 0$ surface, where the wormhole throat is closed. Its radius increases and it crosses the r_- horizon (where the embedding seems again to break). It continues past the r_+ horizon and reaches a maximal radius where it connects to a new parallel region. The complete surface is, of course, described by an infinite chain of identical diagrams. It should be noted that at $r = r_-$ we were careful not to switch between coordinate systems (we have a freedom to connect the vertical lines of the two coordinate systems somewhere between $r = r_-$ and $r = r_+$). The surface is smooth at the point of the coordinate systems' connection ($r = (r_- + r_+)/2 = M = 2$ in this example). Again, the surface is in fact also smooth at $r = r_-$, as a detailed inspection of this area shows.

The timelike wormhole around the singularity is widest (the throat has a radius of r_-) for the hypersurface described by $\xi = 0$. This is similar to the surface described by the horizontal line $v = 0$ in the Kruskal-Szekeres Schwarzschild coordinates (described in figure 1), where the spacelike wormhole is widest (with a throat radius of 2M). When we move in the Kruskal-Szekeres coordinates towards horizontal lines of larger v, the wormhole shrinks until it closes with zero circumference at the $r = 0$ singularity. This resembles our case, where moving the vertical lines towards larger ξ caused the wormhole to shrink until it eventually closed at the hypersurface tangent to $r = 0$. A resemblance between the known Schwarzschild embedding diagrams and the RN embedding diagrams is indeed apparent. Notice again the significant difference that the relevant Schwarzschild surfaces are spacelike and embedded in Euclidean space, whereas our current surfaces are timelike and embedded in Minkowski space. The character of the r_- horizon is different than that of the Schwarzschild event horizon, and this is apparent in the diagrams. In addition, the Schwarzschild spacetime horizontal lines continue towards radial infinity, whereas our vertical lines cross another horizon at r_+ and then reach another wormhole and contract towards r_-. Thus, the resemblance between the Schwarzschild horizontal lines and the RN vertical lines is limited to the region of coordinate system B, describing the area around the singularity and the r_- horizon in the RN spacetime. The portions of the vertical lines that reside in coordinate system A (around the r_+ horizon) are in fact similar to vertical lines in the Schwarzschild spacetime, as is evident by a comparison to figure 2. This is not surprising due to the similarity of coordinate system A to the Kruskal-Szekeres coordinates.

5. Summary

We developed tools and displayed embedding diagrams of spacelike and timelike hypersurfaces of the RN spacetime. The hypersurfaces described provide a typical example of spacelike and timelike slices of the RN spacetime and demonstrate the evolution of RN surfaces. The visualization presented for these slices provides an alternative way to understand intuitively the geometry of the RN spacetime and its properties.

The RN geometry is similar to the Schwarzschild geometry in the region external

to the event horizon ($r > r_+$). In accordance with this the embedding diagrams of hypersurfaces described in the coordinate system that crosses $r = r_+$ were similar to the embedding diagrams of the analogous Schwarzschild hypersurfaces. When we advance in time to different RN spacelike slices described by horizontal lines in this coordinate system, the wormhole shrinks, as is the case when the Schwarzschild spacetime evolves in the time coordinate of Kruskal-Szekeres. However, as expected, when we continue to advance in time and reach the hypersurfaces described in the coordinate system that crosses $r = r_-$, the similarity to Schwarzschild stops. The r_- horizon has no analogy in the Schwarzschild spacetime, and the RN horizontal lines that intersect $r = r_-$ exhibit a different behavior. These hypersurfaces hit on both sides the $r = 0$ singularity, and their geometry near the singularity resembles the geometry of timelike Schwarzschild hypersurfaces, presented as vertical Kruskal-Szekeres lines.

Finally, vertical lines in the RN coordinates describe a path through a wormhole passing beside the singularity. The geometry of the respective surfaces has some features resembling the geometry of the surfaces describing the Schwarzschild wormhole, which are presented there as horizontal lines. The fundamental difference is that the Schwarzschild wormhole is a spacelike path that can not be embarked upon, whereas the RN wormhole is an actual timelike path. This is reflected in the evolution of the spacelike hypersurfaces. When we advance in time the Schwarzschild wormhole shrinks and closes. However, progressing with the RN spacelike surfaces does not cause the wormhole to close, as apparent from our embedding diagrams, and we are not forced to be drained into the singularity. Instead one may choose to take a path like the ones described by our timelike embedding diagrams, and pass through the timelike wormhole to a parallel region and to infinite new universes.

Acknowledgments

We thank Nathalie Deruelle, Joseph Katz and an anonymous referee for helpful remarks. This research was supported by the ISF center of excellence for High Energy Astrophysics and by the Schwartzmann University Chair (TP).

References

[1] Misner C W, Thorne K S and Wheeler J A 1973 *Gravitation* (San Francisco: Freeman)
[2] Chandrasekhar S 1983 *The Mathematical Theory of Black Holes* (Oxford: Oxford University Press)
[3] Graves J C and Brill D R 1960 *Phys. Rev.* **120** 1507
[4] Flamm L 1916 *Physik. Z.* **17** 448
[5] Carter B 1966 *Phys. Lett.* **21** 423